27 August 2015

CURRENT-DEPENDENT INACTIVATION OF THE CATION SELECTIVE ION CHANNELS FORMED BY PEROXIREDOXIN-6 IN LIPID BILAYERS

P. A. Grigoriev[a]
[a]*Institute of Cell Biophysics, Russian Academy of Sciencies, Puschino, Moscow region, 142290, greegorjev@mail.ru*
Graham C. Holt[b]
[b]*Collegium Basilea (Institute of Advanced Study), Basel, Switzerland*

We show that inactivation of cluster ion channels formed by the antioxidant Peroxuredoxin-6 in lipid bilayers is controlled by the amplitude of the ion current. Single ion channels of the oligomer channels cluster including up to 10 mono-channels start to close within several seconds after onset of the membrane voltage if the current is above 40 - 50 pA per single channel of the cluster including up to ten mono-ion channels. Solution of the heat transfer equation for the experimental condition confirms the suggestion about the heat dependence of the observed inactivation.

1 Introduction

Recently we have shown that the 25 kD protein antioxidant Peroxiredoxin-6 forms cation-selective cluster ion channels in the model lipid bi-layer membranes [1]. We have suggested that the observed inactivation of the channels is caused by rising temperature generated by the flow of ions through the channels. Additional experimental data confirming this hypothesis are presented in this article along with the solution of the membrane heat transfer equation for the experimental conditions.

2 Methods

2.1 Experimental

The setup for the lipid bi-layer membranes' formation and classical voltage clump method for measuring membrane currents used in the present study is the same which was used and described in detail in the previous paper [1].

Solid state crystal thermo-resistor type TRA-1 (Russia) having .5 *.5 *1 mm dimensions of the sensor tip was used for temperature measurements of the electrolyte in the vicinity of the circular opening in the teflon wall which was used for the bi-layer formation. These measurements were performed in the absence of the membrane formed.

2.2 Solution heat transfer equation

The temperature surrounding a pore in a membrane immersed in an electrolyte solution is given by the heat transfer equation

$$(\alpha\nabla^2 - \partial_t)u = -q/\rho c_\rho, \tag{1}$$

where $u(r, \theta, \phi, t)$ is the temperature in °K at time t as a function of the spherical coordinates r,θ, ϕ; see Appendix A. Assuming quantum effects due to atomic forces, Van der Waals etc, and convection may be ignored, then the solution to this equation gives the temperature surrounding the pore heated by an electrical current passing through. This current is assumed to exist in a column, pinched at the pore, which has length the distance between the electrodes either side of the membrane. It is assumed that this effectively acts as a point heat source in the centre of the pore, and that the pore represents the region of highest resistance and thus heating, i.e. the heating of the fluid near the electrodes is negligible. The volume of this heating region is defined by the pore and the resistance is discussed in Appendix B. Ambient temperature of the immersed fluid (modelled as water) is taken as 20°C, and the boundary is marked by a sphere of radius $R_0 = 1cm$. The various coefficients of the heat equation are shown in table 1. It is also assumed that the boundary of the fluid volume is held at ambient temperature and acts as an infinite heat sink.

To find the heat generated in the pore, the heat transfer equation is solved in Appendix B with the foregoing assumptions. The solution is dominated

Table 1: Heat transfer equation coefficients.

Coefficient[a]	symbol	units	value
Thermal conductivity	K_c	W/m/°K	0.6
Specific heat capacity	c_ρ	J/Kg/°K	4181.8
Water density	ρ	kg/m^3	10^3
Thermal diffusivity	α	$\alpha = K_c/\rho c_\rho$	1.4 10^{-7}
pore radius	r_0	$nm = 10^{-9}$ m	5
pore depth	r_{0d}	nm	5
boundary radius	R_0	$nm = 10^{-9}$ m	10^7
Power in pore column	P	W	10^{-11}
Current	I	pA	50
pore tunnel resistance [b]	R_{ion}	ohm	1.5 10^4
Power density in pore volume	$q = I^2 R_{ion}/(\pi r_0^2 r_{0d})$	W/m^3	9.61 10^7

[a] Values are for 20°C.

[b] See Appendix B.

by the heating part of the result, equation 15, as shown in the Appendix A figures, 6 and 7, where it is assumed that the pore or cluster channel is an oligomer structure consisting of several monochannels.

3 Results

Characteristic changes of the membrane current in the presence of Peroxiredoxin-6 are shown in Fig. 1 Differences in the steps of the increasing current can be attributed either to difference in the diameter of the opening conducting channels or to the different number of simultaneously opened single channels.

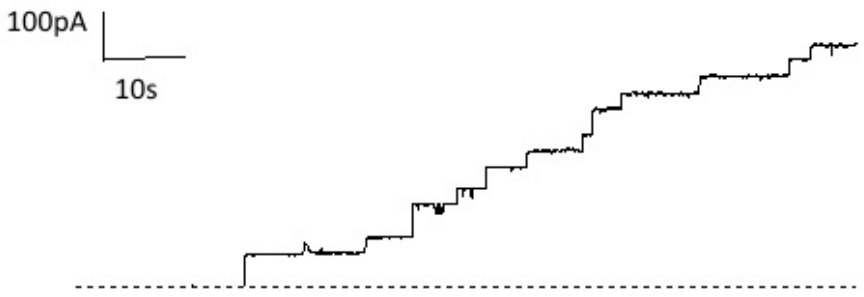

Figure 1: Characteristic increase of the current in presence of Prx-6at both sides of the membrane. Conditions: 5*10 -8 M Prx-6, 200 mM KCl, V = 27 mV.

The recordings shown in Fig. 2 suggest that the second option is more probable. Indeed, the mono-channels with conductance of about 500 +- 50 pS are being revealed at higher voltages when oligomer ion clusters start to inactivate step by step at 95 and 138 mV, Fig. 2. Closing of monochannels of the cluster channel (which are assumed to be a bundle of such mono- or single channels) are shown with several seconds of dwell times in the open state. Closing is observed when the amplitude of the current rises above about 40 pA per single channel member of the bundle, and the inactivation is faster

at higher currents. The current of the ion channels but not the membrane

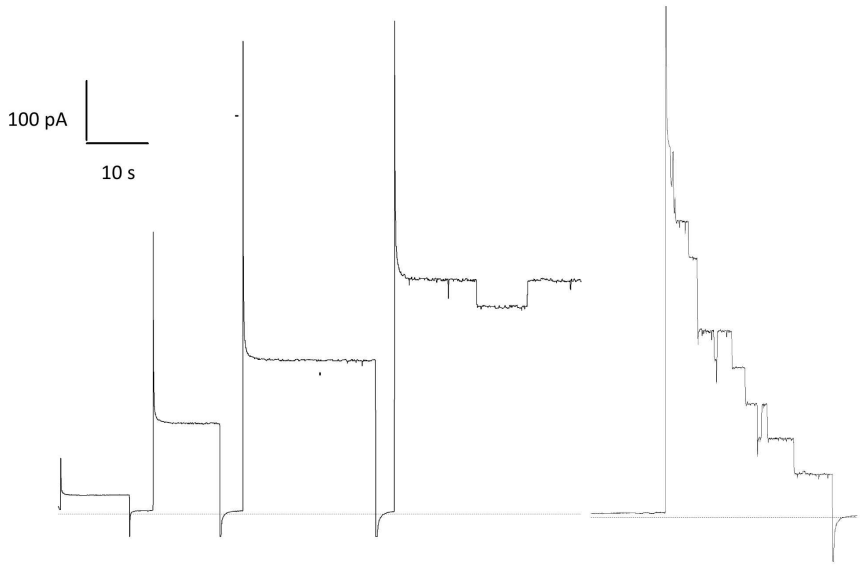

Figure 2: Effect of the voltage (current) increase on the appearance of the inactivation of the cluster channels. Conditions: voltages for the recorded currents: 15, 42, 66, 95 and 138 mV. 200 mM KCl. Opened ion cluster channel includes up to 10 mono-channels being closed at higher voltages (currents).

voltages induces the cluster channel inactivation as follows from the data presented in Fig. 3, where recordings of the currents through a pentamer cluster channel at the condition of 300 / 100 mM of KCl concentration gradient are shown. Describing Fig.3 in detail: there was 100 mM KCl at both sides of the membrane at the start of the recording , then a sample of KCl is added into the cis- side to create 3 to1 concentration gradient across the membrane. The rather noisy part at the start of the trace with increasing current is due to the developing KCl gradient when the external DC voltage is zero. The level of the gradient driven current can be either a or b depending on the dynamic nature of the number of mono-channels in the cluster. Further we see that inactivation takes place only when the current, not voltage, is high enough. It is again, as with Fig.2, at about 40 pA per single channel. Let us consider 1 part of the trace. Here the applied membrane voltage is changed

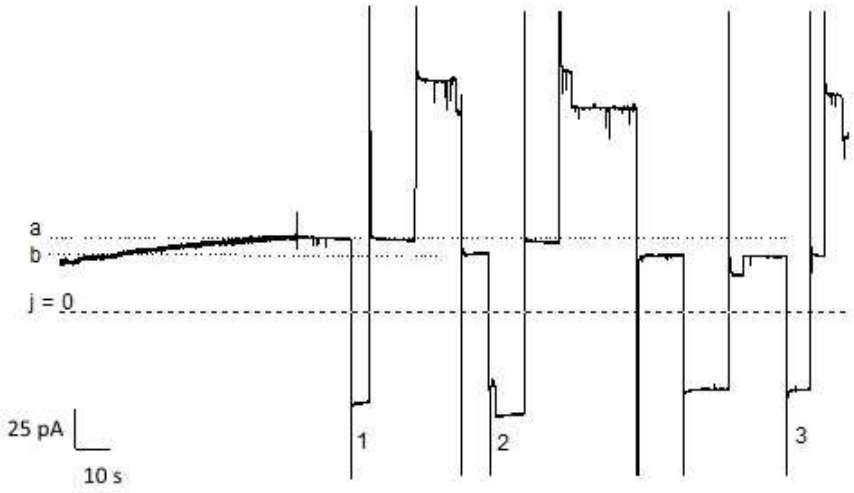

Figure 3: Inactivations of the cluster channels in the conditions of 300 /100 mM KCl gradient across the bilayer. The inactivation takes place only when the current generated by the KCl gradient is summed up with the DC voltage driven current. Indeed, the inactivation steps down are recorded at + 54 mV but not at - 54 mV (a part of the trace started at 1). The same behaviour of the cluster channel is observed at +- 58 mV and +- 64 mV (parts 2 and 3 of the recording.

from 54 to 0 and then to +54 mV. Positive and negative voltages are equal, so the amplitude of the electric field inside of the membrane is the same i.e. it does not depend upon the KCl concentration gradient. We see that the inactivation is registered only at +54 mV when the external DC voltage and gradient currents are summed up. The currents are subtracted at -54 mV. The similar behaviour of the channels in the cluster are observed at 2 and 3 regions of the trace. Current voltage (I-V) characteristic of the ion cluster channels is linear and symmetric (there is no rectification) as was shown in our previous paper [1]. Therefore we can expect that similar behavior of the membrane currents would be observed for the reversed KCl concentration gradient across the membrane. Additional experimental results confirming the hypothesis of the thermal nature of the inactivation are shown in Fig.4 where the rise of the electrolyte temperature at about 1mm distance from the central point of the circular hole in the teflon wall used for the support of the lipid bilayer membrane is shown. The test is conducted without the membrane formed. Electric power pressure at the sphere with 30 nm radius in the conditions of the Fig.2 experiment was about 10^{-14} W/ nm^2 (100 pA and 100 mV as average amplitudes of the ion current and membrane voltage are taken for the calculation). The same power pressure at the surface of 1mm radius sphere was generated in the Fig.4 experiment. The temperature is rising at about 20 °C /s . Therefore it is quite reasonable to expect that the temperature of the ion conducting complexion channel cluster can be high enough to cause the inactivation.

4 Discussion

We show that the Prx-6 channels are modelling excitable cell membrane ion channels much better then gramicidin and alamethicin antibiotics widely used in similar studies. The main properties of the Prx-6 channels are: high K/Cl selectivity (more then 100), cluster organization like in the cell membranes [3], and well defined inactivation similar to that of the cell membrane's channels . The inactivation characterized in our paper is current-dependent, but not as voltage - dependent as described in the work of Hodgkin and Huxley [5]. Moreover, this observed contradiction correlates with the quotation from the paper of Shimon Marom and L F. Abbott [6]: "The general approach developed by Hodgkin and Huxley (1952) over 40 years ago to describe sodium and potassium currents in the squid giant axon has been successfully applied to many other membrane currents and now forms the basis for virtually all modelling studies of neuronal behavior. However, further research has clearly

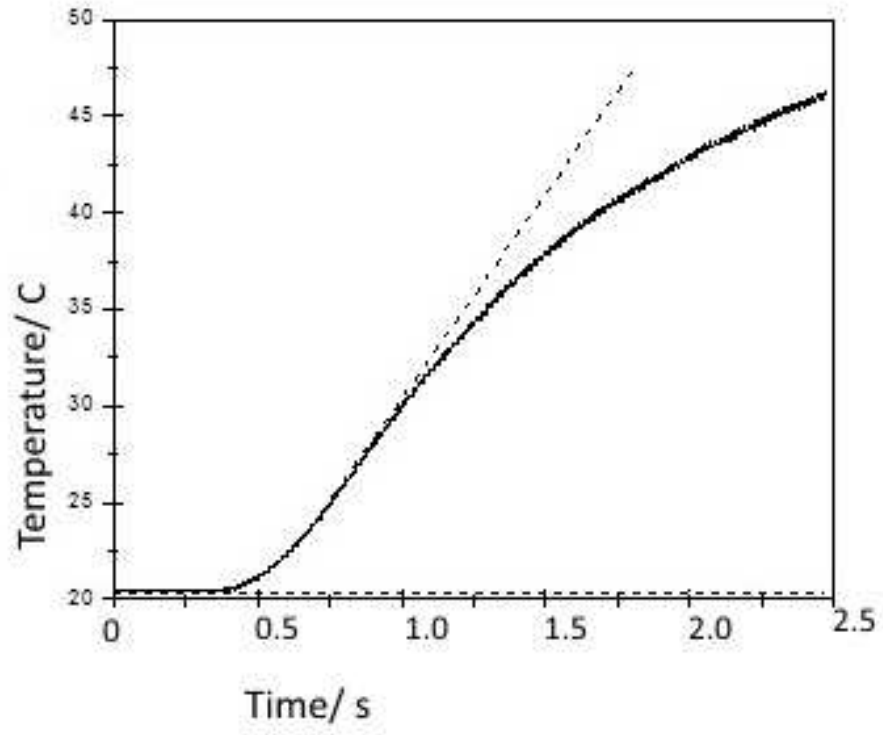

Figure 4: Temperature of the electrolyte at a about 1 mm from the plane were the bilayer would be formed. Conditions: 2 M NaCl. Power pressure at the surface of the 1 mm radius sphere with center at the mid-point of the hole is about 10^{-14} W/ nm^2 .

demonstrated that the behaviour of membrane channels is often inconsistent with the general assumptions of the Hodgkin-Huxley formalism". Therefore the results of the model experiments with Prx-6 ion channels might be valuable for understanding the physics of the inactivation phenomena in nerve cells.

A Appendix: Heat Transfer Solution

The coordinate system is shown in figure 5 with r_0 the pore radius and an outer boundary R_0 at ambient temperature. The heat transfer equation is

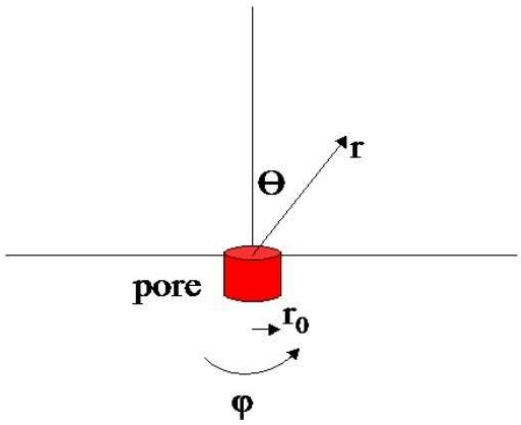

Figure 5: Solution space coordinate system

given by

$$(\alpha\nabla^2 - \partial_t)u = -q/\rho c_\rho, \tag{2}$$

where $u(r, \theta, \phi, t)$ is the temperature in °K, and $\alpha = K_c/\rho c_\rho$. The boundary conditions are:

$$u(r = R_0, \theta, \phi, t = 0) = 293 \tag{3}$$

and

$$u(r = R_0, \theta, \phi, t) = 293. \tag{4}$$

The system is spherically symmetric and independent of θ and ϕ. Moreover, this partial differential equation has a time dependent forcing function so that Duhamel's method provides a solution by solving the alternative equation

$$(\alpha\nabla^2 - \partial_t)\Psi(r, t, \tau) = -g(r, \tau). \tag{5}$$

Then the solution is given by the integral

$$u(r,t) = u_0 + \int_{\tau=0}^{t} \partial_t \Psi(r, t-\tau, \tau) d\tau, \tag{6}$$

where

$$(\alpha \nabla^2 - \partial_t)\Psi(r,t,\tau) = 0 \tag{7}$$

and condition

$$\partial_t \Psi(r=0, t=0) = -g. \tag{8}$$

This equation, 7, has solution by separation of variables. For the heat transfer equation $g = q/\rho c_\rho$ and the boundary conditions 3, 4 become:

$$\Psi(r = R_0, t = 0) = 0 \tag{9}$$

and

$$\Psi(r = R_0, t) = 0. \tag{10}$$

Returning to equation 7 and solving by separation of variables gives

$$\Psi = e^{-\lambda t} R(r, \theta, \phi) \tag{11}$$

where $R(r, \theta, \phi)$ satisfies Helmholtz's equation and for $\gamma = \pm\sqrt{\lambda/\alpha}$

$$R = \sum_{l=0}^{\infty} \sum_{m=-1}^{l} [a_{ml} j_l(\gamma r) + b_{ml} y_l(\gamma r)] Y_l^m(\theta, \phi). \tag{12}$$

Here $j_l(x)$ and $y_l(x)$ are Bessel functions and $Y_l^m(\theta, \phi)$ the spherical harmonics.
By spherical symmetry $m = 0$ and boundary condition 9 is satisfied for

$$\gamma_n = n\pi/R_0 \tag{13}$$

for $n \geq 1$ with $l = 0$. The solution is thus

$$\Psi = \sum_{n=1}^{\infty} e^{-\lambda_n t} a \sin(\gamma_n r)/\gamma_n r. \tag{14}$$

Condition 8 then gives $a = g/(\alpha\gamma_1^2)$ and after integration in equation 6, noting boundary condition 10, yields the solution

$$u(r,t) = 293 + \int_{\tau=0}^{t} [\partial_t \hat{\Psi}(r, t-\tau, \tau)] d\tau$$

$$= 293 + \mathrm{q}/(\rho c_\rho \alpha \gamma_1^2) \sum_{n=1}^{\infty} [1 - e^{-\lambda_n t}] \sin(\gamma_n r)/(\gamma_n r). \tag{15}$$

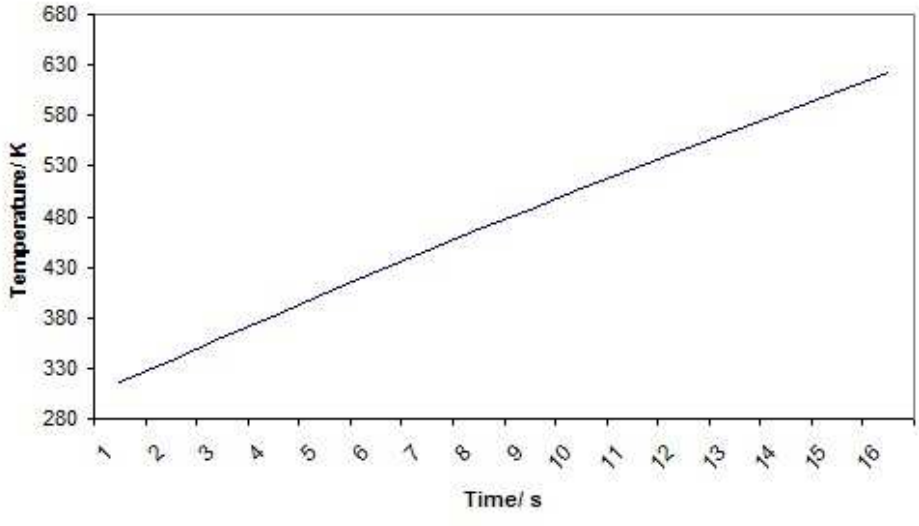

Figure 6: Temperature vs time at radius $r = 100nm$

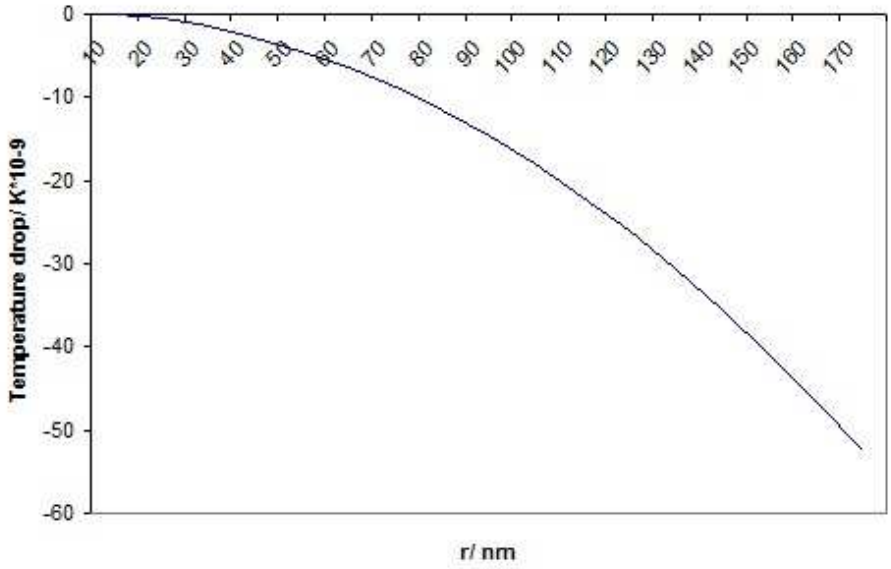

Figure 7: Temperature drop vs radius at time $t = 5s$

B Appendix: Equivalent circuit model

The experimental set up is represented in figure 8 with the equivalent circuit for an active membrane pore in a dilute electrolyte of KCl. Diffusion through the pore results in a battery effect, the Nernst potential, as only ions pass through. Resistance of the elements of the circuit formed from the electrolyte may then be calculated using the conductance, σ of 2M KCl in water.

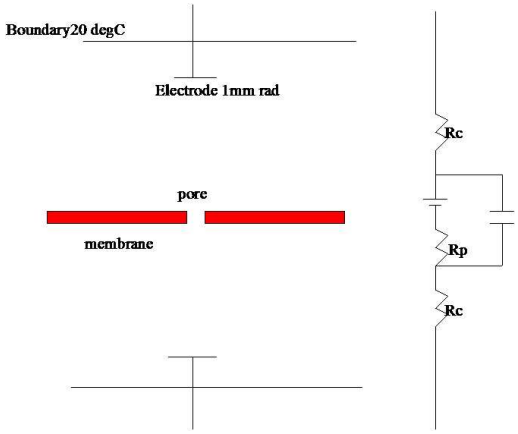

Figure 8: Measurement set up

The half column resistance is given by the integral,

$$R_c = \int_{r_{0d}/2}^{l_c/2} [1/(\sigma\pi(z tan^2\theta)]dz \tag{16}$$

$$= (2/r_{0d} - 2/l_c)/(\sigma\pi), \tag{17}$$

where $\tan\theta = r_e/(l_c/2)$.

The equivalent circuit resistances are shown in table 2. The effective resistance is orders of magnitude greater than the sum of $R_p + 2R_c$. Thus an I^2R_p calculation for power dissipated in the fluid is suspect.

However, the resistance in the pore from measurement must be much greater which leads to consideration of quantum effects to explain the discrepancy.

At the quantum level, the effective pore resistance may be altered by electron tunnelling through the pore. The one dimensional Nernst-Planck equation

Table 2: Equivalent circuit resistances.

Circuit element[a]	symbol	units	value
conductance 2M KCl	σ	siemens	2 10^4
electrode radius	r_e	nm	1 10^6
electrode spacing	l_c	nm	2 10^7
half column resistance	$R_c = (2/r_{0d} - 2/l_c)/(\sigma\pi)$	ohm	6.3 10^5
pore depth	r_{0d}	nm	5
pore resistance	$R_p = r_{0d}/(\sigma\pi r_0^2)$	ohm	3.2 10^3
voltage applied	V	mV	200
current measured	I	$pA = 10^{-12}$ A	50
effective resistance	$R_{tot} = V/I$	ohm	4 10^9

[a] Values are for 20°C.

gives the current density

$$j = -q_{ion}D[\frac{dn(z)}{dz} + q_{ion}n(z)/(K_B u_0)\frac{d\phi(z)}{dz}], \tag{18}$$

where q_{ion} is the ion density, D is the diffusion coefficient, K_B is the Boltzmann constant, n(z) is the ion density and $\phi(z)$ is the potential difference across the pore. Assume the potential difference is linear and tunnelling occurs, so that

$$\phi(z) = Vz/r_{0d} + \delta V, \tag{19}$$

where δV is the tunnelling potential. The capacitance C_p of the pore with charge Q_{pore} acts as a potential barrier, with energy $Q_{pore}^2/(2C_p)$. Then with the addition of a tunnelling electron this becomes

$$(|Q_{pore}| - |e|)^2/(2C_p), \tag{20}$$

and this state is maintained if it is less than the existing energy, i.e.

$$(|Q_{pore}| - |e|)^2/(2C_p) \leq Q_{pore}^2/(2C_p) \tag{21}$$

$$orV \geq e/(2C_p); \tag{22}$$

noting that V=Q_{pore}/C_p. Thus taking $\delta V = e/(2C_p)$ensures tunnelling occurs. Equation 18 may be solved after some integration [7] to give the current through the pore as

$$I = -2\pi r_0^2 j \tag{23}$$

$$= -2\pi r_0^2 q_{ion}^2 nDV/(r_{0d}K_B u_0)e^{-q_{ion}\delta V/(K_B u_0)}. \quad (24)$$

The effective pore resistance is then for tunnelling

$$R_{ion} = r_{0d}K_B u_0/(2\pi r_0^2 q_{ion}^2 nD)e^{q_{ion}e/(2C_p K_B u_0)}. \quad (25)$$

Ions remaining in the pore effectively reduce current flow, i.e. Coulomb block. These ions have entropy

$$\Delta S = K_B ln(nVol), \quad (26)$$

where Vol is the pore volume, and result in a potential of $u_0\Delta S/q_{ion}$, namely

$$\delta V_{block} = K_B u_0 ln(nVol)/q_{ion}. \quad (27)$$

Substituting for δV in equation 24 then gives

$$R_{block} = r_{0d}K_B u_0/(2\pi r_0^2 q_{ion}^2 nD)nVol. \quad (28)$$

Table 3 shows the various constants used to define the pore resistance from quantum principles. From equation 2, the rate of change of temperature near the pore is

$$\partial_t u = q/\rho c_\rho. \quad (29)$$

and then Table 4 shows rate of change of temperature.

The quantum approach gives good agreement with the block resistance but for tunnelling is particularly sensitive to C_p and thus absolute values may vary significantly. Nevertheless the tunnelling resistance gives heating rates in agreement with experiment.

Table 3: Quantum derived resistances.

Constant	symbol	units	value
Diffusion coefficient water[a]	D	m^2/s	1.8 10^{-9}
electron charge	e	coulombs	1.6 10^{-19}
ionic charge[b]	q_{ion}	coulombs	1.6 10^{-19}
Boltzmann constant	K_B		1.38 10^{-23}
ion density 2M	n = 2.6 $10^{23}10^3$	number/m^3	1.2 10^{27}
capacitance[c]	C_p	F	6.28 10^{-19}
block resistance	R_{block}	ohm	1.1 10^9
tunnel resistance	R_{ion}	ohm	1.5 10^4

[a] see [8], u_0=293.

[b] valence potassium=1 so $q_{ion} = e$

[c] 0.8 $\mu F/cm^2$ see [9]

Table 4: Heating rates.

Tunnelling power	key parameter	rate °C/s
I^2R_{ion}	C_p	23

C References

1. Grigoriev P.A. , Sharapov M.G. and Novoselov V.I. Properties of ion channels formed by peroxredoxin-6 in the lipid bilayers: claster channel inactivation. JBPC, 2014. V 14, N 3, pp.54 - 5

2. Mikkola R, Andersson MA, Kredics L, Grigoriev PA, Sundell N, Salkinoja-Salonen MS. 20-Residue and 11-residue peptaibols from the fungus Trichoderma longibrachiatum are synergistic in forming Na+/K+ -permeable channels and adverse action towards mammalian cells. FEBS J. 2012 Nov;279(22):4172-90. doi: 10.1111/febs.12010. Epub 2012 Oct 16.

3. Kole MJ, Qian J, Waase MP, Klassen TL, Chen TT, Augustine GJ, Noebels JL. Selective Loss of Presynaptic Potassium Channel Clusters at the Cerebellar Basket Cell Terminal Pinceau in Adam11 Mutants Reveals Their Role in Ephaptic Control of Purkinje Cell Firing.J Neurosci. 2015 Aug 12;35(32):11433-44. doi: 10.1523/JNEUROSCI.1346-15.2015.

4. Cole K.S., Moore J.W. Ionic current measurements in the squid giant axon membrane. J.Gen. Physiol. 1960 Sep; 44: 123-67.

5. Hodgkin A.L. and Huxley A.F. A quantitative description of membrane current and its application to conduction and excitation in nerve. J.Physiol. 1952, 117, 500-544

6. Marom S, Abbott LF. Modeling state-dependent inactivation of membrane currents. Biophys J. 1994 Aug;67(2):515-20.

7. A Meyertholen, M Di Ventra; Quantum Analogies in Ionic Transport Through Nanopores, arXiv:1305.7450v1 [cond-mat.mes-hall] 31 May 2013 http://arxiv.org/abs/1305.7450

8. V.M. Lobo et al; Diffusion Coefficients in Aqueous Solutions of Beryllium Sulfate at 298 K, J. Chem. Eng. Data 1994,39, 726-728

9. B. Hille; Ion Channels of Excitable Membranes, Sinauer Assoc., 2001, http://pub.ist.ac.at/Pubs/courses/2012/introductiontoneuroscience1/docs/Lectures May 13,15/Hille Ion Channels of Excitable Membranes Chapter1.pdf